Molecular Therapy
Original Article

Susceptibility to Cardiac Arrhythmias and Sympathetic Nerve Growth in VEGF-B Overexpressing Myocardium

Johanna Lähteenvuo,[1,5] Olli-Pekka Hätinen,[1,5] Antti Kuivanen,[1] Jenni Huusko,[1] Jussi Paananen,[1] Markku Lähteenvuo,[1] Jussi Nurro,[1] Marja Hedman,[2] Juha Hartikainen,[2] Nihay Laham-Karam,[1] Petri Mäkinen,[1] Markus Räsänen,[3] Kari Alitalo,[3] Anthony Rosenzweig,[4] and Seppo Ylä-Herttuala[1,2]

[1]A.I. Virtanen Institute for Molecular Sciences, University of Eastern Finland, Yliopistonranta 1E, 70211 Kuopio, Finland; [2]Heart Center, Kuopio University Hospital, Puijonlaaksontie 2, 70210 Kuopio, Finland; [3]Wihuri Research Institute and Translational Cancer Medicine Program, Faculty of Medicine, University of Helsinki, Haartmaninkatu 8, 00290 Helsinki, Finland; [4]Massachusetts General Hospital, 55 Fruit Street, Boston, MA 02114, USA

VEGF-B gene therapy is a promising proangiogenic treatment for ischemic heart disease, but, unexpectedly, we found that high doses of VEGF-B promote ventricular arrhythmias (VAs). VEGF-B knockout, alpha myosin heavy-chain promoter (αMHC)-VEGF-B transgenic mice, and pigs transduced intramyocardially with adenoviral (Ad)VEGF- B186 were studied. Immunostaining showed a 2-fold increase in the number of nerves per field (76 vs. 39 in controls, $p < 0.001$) and an abnormal nerve distribution in the hypertrophic hearts of 11- to 20-month-old αMHC-VEGF-B mice. AdVEGF-B186 gene transfer (GT) led to local sprouting of nerve endings in pig myocardium (141 vs. 78 nerves per field in controls, $p < 0.05$). During dobutamine stress, 60% of the αMHC-VEGF-B hypertrophic mice had arrhythmias as compared to 7% in controls, and 20% of the AdVEGF-B186-transduced pigs and 100% of the combination of AdVEGF-B186- and AdsVEGFR-1-transduced pigs displayed VAs and even ventricular fibrillation. AdVEGF-B186 GT significantly increased the risk of sudden cardiac death in pigs when compared to any other GT with different VEGFs (hazard ratio, 500.5; 95% confidence interval [CI] 46.4–5,396.7; $p < 0.0001$). In gene expression analysis, VEGF-B induced the upregulation of Nr4a2, ATF6, and MANF in cardiomyocytes, molecules previously linked to nerve growth and differentiation. Thus, high AdVEGF-B186 overexpression induced nerve growth in the adult heart via a VEGFR-1 signaling-independent mechanism, leading to an increased risk of VA and sudden cardiac death.

INTRODUCTION

Cardiac deaths account for 39% of deaths in Europe and the United States, and in over 90% of the cases, the underlying cause is ischemic heart disease. Sprouting of sympathetic nerve endings in the peri-infarct zone and increased sympathetic activation play a role in this pathologic process.[1] Sympathetic nerves follow the course of coronary vessels on the epicardial surface and extend into the ventricular myocardium. Nerve sprouting can be observed within days after ischemic myocardial injury.[2] An increase in nerve density and an imbalance in the distribution pattern of nerves in the myocardium has been shown to lead to an increased susceptibility to arrhythmias and even sudden cardiac death.[3] However, molecular mechanisms underlying the rapid modulation of cardiac innervation after myocardial ischemia are unknown, and no specific therapies exist. Both stimulatory signals, such as nerve growth factor (NGF) secreted from macrophages and fibroblasts, and negative regulation under basal conditions by Sema3a, a neuropilin (Nrp)-1 receptor ligand, have been suggested.[2,4,5]

Nerve and blood vessel development and growth occur in parallel and share many molecular regulators. Vascular endothelial growth factors (VEGFs) regulate blood vessel growth both during development and in adult tissues via VEGF receptors (VEGFRs) and Nrp receptors.[6] We have previously shown that VEGF-B induces tissue-specific angiogenic responses in the myocardium and upregulates Nrp-1 expression.[7] VEGF-B has also been recently linked to nerve growth in the retina,[8] and it has been shown to protect neurons from ischemic injury in brain.[9] The mechanism of VEGF-B induced nerve growth, and protection has been suggested to be mediated by both VEGFR-1 and Nrp-1,[10] based mainly on receptor expression on neurons, but the molecular mechanism remains unknown.

Here, we show that high levels of VEGF-B generated by transgenic or adenoviral (Ad) overexpression can induce sympathetic nerve sprouting in the myocardium, which can increase the risk of ventricular arrhythmias (VAs) and sudden cardiac death. Administration of an Ad vector encoding soluble Nrp-1 (AdsNrp1) further increased the nerve sprouting. Interestingly, co-transduction with soluble decoy

Received 31 July 2019; accepted 13 March 2020;
https://doi.org/10.1016/j.ymthe.2020.03.011.

[5]These authors contributed equally to this work.

Correspondence: Seppo Ylä-Herttuala, MD, PhD, FESC, A.I. Virtanen Institute for Molecular Sciences, University of Eastern Finland, Yliopistonranta 1E, 702100 Kuopio, Finland.
E-mail: seppo.ylaherttuala@uef.fi

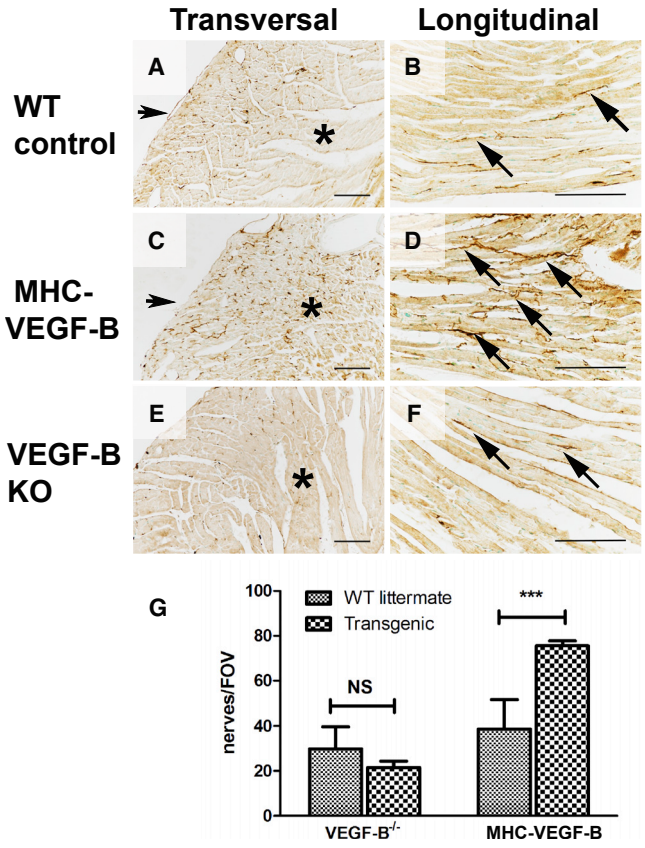

Figure 1. Genetic Overexpression of VEGF-B Increases Nerve Density in the Female Mouse Heart and Disturbs the Transmural Patterning of Sympathetic Nerve Innervation

GAP 43 staining (brown) was used to detect nerve endings in the mouse myocardium (11 to 20 weeks old). (A) Nerve structure and density were normal in control mice (n = 6). Nerves were mainly located in the epicardium, and density was much lower in the mid-myocardium (asterisk). (B) Nerve fibers (arrows) ran parallel to muscle fibers in the control myocardium, and a few branching points were observed. Nerve distribution was normal, as nerve density was greater in the epicardium (bottom) and became sparser in the mid-myocardium (top). (C) Genetic overexpression of VEGF-B increased the total number of nerve endings (n = 6). Nerve density gradient was disturbed, and nerve fibers were also observed in the mid-myocardium (asterisk). (D) Increased density of nerve endings, aberrant anatomic structure, and increased branching of nerves (arrows) were observed in the αMHC-VEGF-B mice. A normal gradient of nerve density was missing. (E) Nerve density and patterning were not significantly reduced in VEGF-B KO mice, indicating that VEGF-B is not essential for sympathetic patterning during development (n = 6). (F) Nerve morphology in VEGF-B KO mice was normal (arrows). (G) Nerves were visualized using GAP43 immunostaining, and nerve density was calculated from transverse sections. Results are expressed as nerve endings per FOV. Nerve density was significantly increased in αMHC-VEGF-B mice as compared to WT controls (1.9-fold, $p < 0.001$) but was not significantly different in VEGF-B KO mice; not significant (NS) as compared to WT controls. Scale bars, 100 μm.

VEGFR-1 (sVEGFR-1) increased the incidence of arrhythmias. Expression of Nr4a2, AFT6, and MANF, molecular mediators of nerve growth, was increased concomitantly in the myocardium and, thus, may explain the pathogenic basis of the findings.

RESULTS

VEGF-B Regulates Sympathetic Innervation of the Heart during Development

Without adrenergic stress, the alpha myosin heavy-chain promoter (αMHC)-VEGF-B transgenic mice, which overexpress VEGF-B in cardiomyocytes, show about a 2-fold increased coronary vessel density, non-pathological cardiac hypertrophy, and a normal sinus rhythm and lifespan. Furthermore, they do not show increased mortality after myocardial infarction induced by ligation of the left anterior descending coronary artery (10 versus 21 of a total of 130 mice).[11] Immunostaining of the ventricular walls of αMHC-VEGF-B mice showed more GAP43-positive nerves than in the wild-type (WT) littermate control mice (cf. Figures 1A and 1C). In addition, they had a dense network of nerve fibers in the mid-myocardium and endocardium, unlike in the control mice, where a clear gradient from epicardium to endocardium was observed (cf. Figures 1A and 1C). The nerves also appeared more branched and tortuous in longitudinal sections (Figure 1D). In young mice (7–10 weeks old), nerve densities did not reach statistical differences; however, it became significant in older mice (11–20 weeks old) (Figure S1). The nerve density was 2-fold higher in older αMHC-VEGF-B mice than in WT control littermates (76 versus 39 GAP43-positive nerve endings per field of view [FOV]; $p < 0.001$) (Figure 1G), suggesting that myocardial innervation remains plastic and responsive to VEGF-B stimulation in adult mice.

As GAP43 is a general marker of sprouting nerve endings,[5,12] the sympathetic nature of the nerve endings was confirmed by tyrosine hydroxylase (TH) staining (Figure S2). Whole-mount TH stainings revealed a denser, more branched network of sympathetic nerves on the epicardial surface of the αMHC-VEGF-B hearts than that on the hearts of WT controls or VEGF-B knockout (KO) mice (Figure S3). The nerve ending density and length were similar in WT and VEGF-B KO mice (Figure 1E), suggesting that the lack of VEGF-B does not significantly impair sympathetic nerve growth in the heart (Figures 1E–1G).

Ad Overexpression of VEGF-B Leads to Nerve Sprouting in the Heart

Ad overexpression of VEGF-B_{186} led to the sprouting of nerve endings in the injection area in both normoxic and ischemic pig myocardia after 6 days of gene transfer (GT) (Figure 2). Nerve density was higher, and the nerves appeared more branching and tortuous in AdVEGF-B_{186}-transduced hearts than in AdLacZ control hearts (cf. Figures 2A and 2C; cf. Figures 2B and 2D), and dense arborizations were observed especially in fibrous tissue and around the blood vessels (insert in Figure 2D). The nerves were sympathetic based on their location and staining for TH (Figure S4). Stimulation of nerve growth was not dependent on VEGFR-1 signaling, as co-transduction of AdVEGF-B_{186} with sVEGFR-1 (AdsVEGFR-1) did not significantly alter the density of nerve endings when compared to transduction with AdVEGF-B_{186} alone (cf. Figures 2E and 2F with Figures 2C and 2D).

Surprisingly, co-transduction with AdsNrp-1 significantly increased both nerve density and branching when compared to transduction

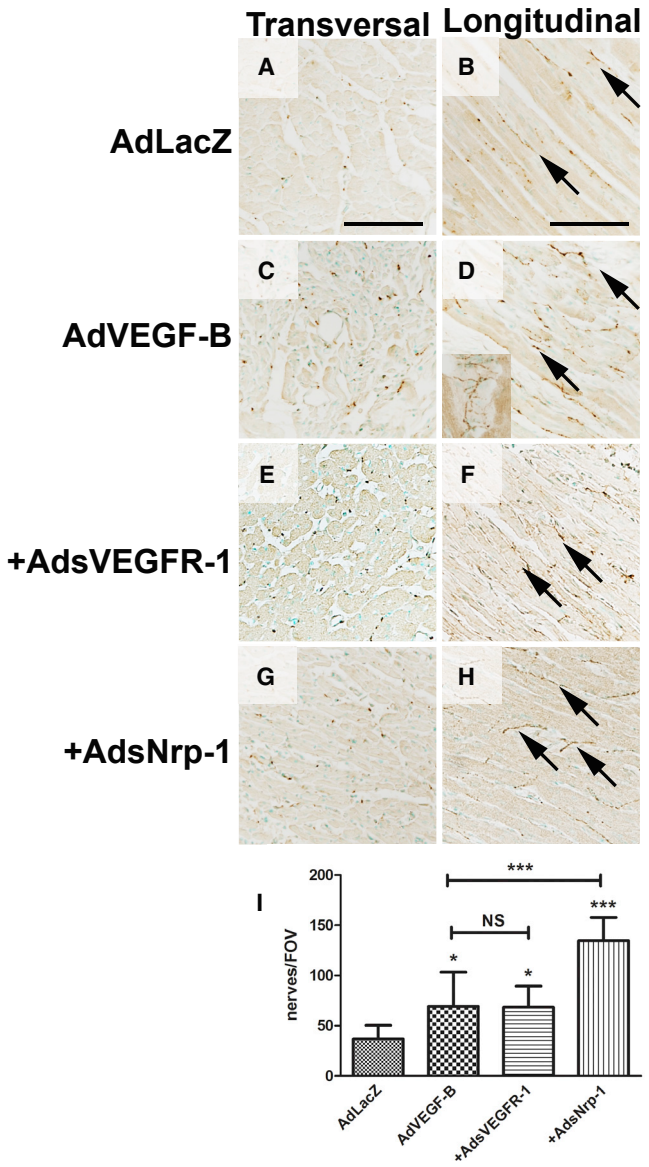

Figure 2. Ad Overexpression of VEGF-B_{186} Stimulates Nerve Growth in Normoxic Adult Pig Myocardium with VEGFRs Modulating Nerve Growth

(A and B) Nerve density (A) and structure (B) were normal in AdLacZ-transduced pig myocardium (n = 4) 6 days after GT. Nerves ran parallel to muscle fibers, and a few branching points were observed (arrows). (C) AdVEGF-B_{186} induced rapid nerve sprouting and increased nerve density in the myocardium 6 days after GT (n = 5). (D) Nerve endings appeared tortuous, and more branching points were observed in AdVEGF-B_{186}-transduced hearts (arrows). Nerve branching was apparent, especially in the connective tissue surrounding blood vessels (insert). The role of known VEGF-B receptors VEGFR-1 and Nrp-1 were studied using co-transductions of adenovirally overexpressed soluble receptors. (E) Overexpression of soluble VEGFR-1 (AdsVEGFR-1) in combination with AdVEGF-B_{186}, did not significantly alter nerve density in the myocardium as compared to AdVEGF-B_{186} alone, suggesting that the induction of nerve growth was not mediated by native, cell-membrane-bound VEGFR-1. (F) Nerve morphology was also comparable to AdVEGF-B_{186}. (G) In contrast, co-transduction with AdsNrp-1 increased nerve density in the GT area as compared to VEGF-B_{186} alone. (H) AdsNrp-1 also increased nerve ending branching, and more transversally running nerve endings were visible. (I) Quantification of nerve density in the transduced myocardium revealed that both AdVEGF-B_{186} and AdVEGF-B_{186}+AdsVEGFR-1 increased nerve density in the myocardium as compared to AdLacZ control (1.8-fold, $p < 0.05$ in both groups). AdsVEGFR-1 did not significantly alter the nerve density as compared to AdVEGF-B_{186} alone. In contrast, AdsNrp-1 significantly increased nerve density as compared to AdVEGF-B_{186} alone (1.8-fold, $p < 0.001$). NS, not significant.

with AdVEGF-B_{186} alone (cf. Figures 2G and 2H with Figures 2C and 2D). Whereas VEGFR-1-mediated signaling did not appear essential for nerve sprouting, VEGF-B and soluble Nrp-1 may interfere with endogenous inhibition of nerve growth. VEGF-B competes for binding to Nrp-1 with endogenous inhibitory ligands such as Sema3a, and sNrp-1 may further enhance this effect (shown later in Figure 4A).

The number of GAP43-positive nerve endings in AdVEGF-B_{186}-transduced hearts was 1.8-fold higher than in AdLacZ control hearts (Figure 2I; 141 versus 78 nerve endings per FOV, $p < 0.05$). AdsVEGFR-1 did not alter nerve density as compared to AdVEGF-B_{186} alone, while AdsNrp1 alone significantly increased nerve density ($p < 0.001$). In ischemic hearts, an increase in nerve density was also observed in the infarction border zone after AdVEGF-B_{186} gene transfer (data not shown). These results indicate that cardiac nerves are highly plastic and start to sprout in the adult heart when the Nrp-1 receptor is overexpressed in the heart.

VEGF-B Overexpression and Increased Nerve Density Lead to Arrhythmias and Sudden Cardiac Death

Transgenic VEGF-B overexpression and increased nerve density were associated with susceptibility to VA during dobutamine-induced adrenergic stress (Figure 3). Ten min after intraperitoneal (i.p.) injection of 1 mg/kg dobutamine, 60% of the αMHC-VEGF-B mice had arrhythmias as compared to 7% in WT controls (Figure 3A). The effect of dobutamine began to diminish after 10 min. It should be noted, however, that in the αMHC-VEGF-B mice, the increased coronary vessel density may increase the exposure of cardiomyocytes to dobutamine and that cardiac hypertrophy has also been reported to increase the frequency of arrhythmias.[11,13,14]

In electrocardiogram (ECG) analysis, no arrhythmias were observed in any of the pigs at baseline (data not shown). Only occasional ventricular extrasystoles were observed in 1 out of 7 ischemic AdLacZ control pigs and in 1 out of 7 normoxic AdVEGF-B_{186} pigs (Figure 3B). AdsVEGFR-1 increased the risk of arrhythmias, as 1 out of 4 normoxic pigs and 6 out of 6 ischemic pigs displayed ventricular tachycardias, frequent ventricular extrasystoles, and even sustained tachycardia, ventricular fibrillation (VF), and sudden cardiac death, suggesting that increased nerve ending density increased the risk of malignant arrhythmias (Figure 3B). Rhythm monitors were implanted in a subset of pigs to characterize the arrhythmias further and to determine the cause of death. A representative ECG recording of a sustained ventricular tachycardia, eventually leading to VF in an

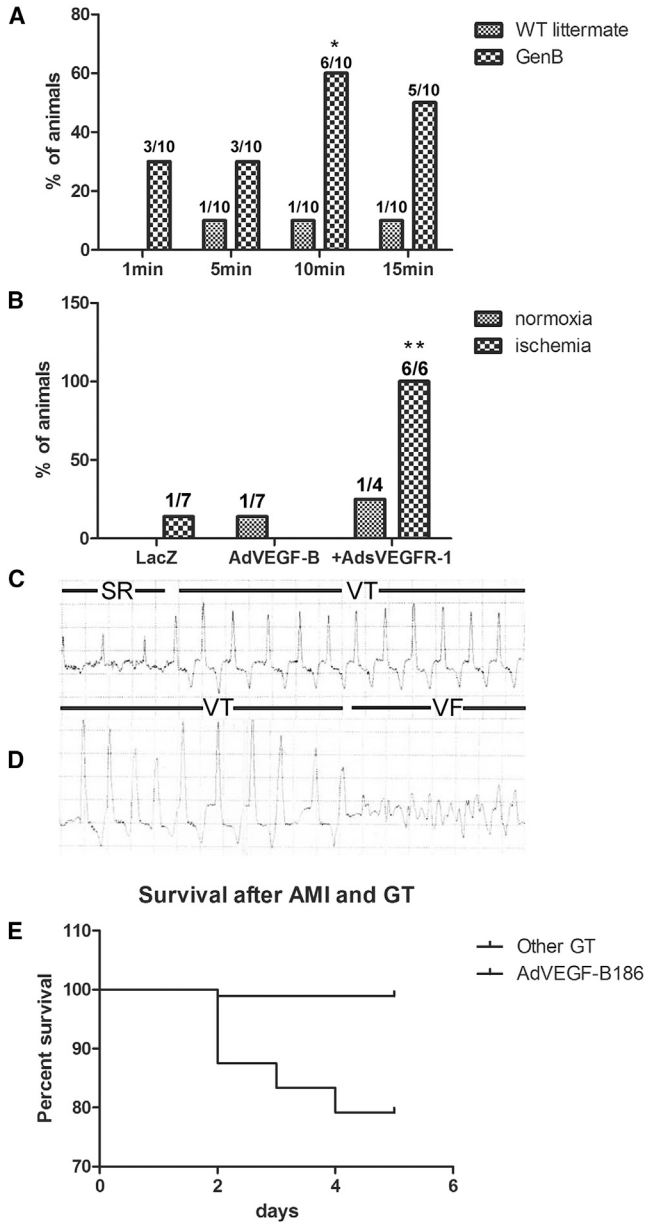

Figure 3. VEGF-B_{186} Overexpression Increases Susceptibility to Ventricular Arrhythmias

(A) αMHC-VEGF-B mice (n = 10) were more susceptible to arrhythmias during dobutamine stress. 60% of animals displayed arrhythmias 10 min after i.p. dobutamine injection ($p < 0.05$), suggesting that these mice were more sensitive to sympathetic stimulation. (B) Arrhythmias were also observed after Ad overexpression of VEGF-B_{186}. ECGs were recorded on day 6 after GT. Ventricular extrasystoles and non-sustained VTs were observed in only one AdLacZ control after acute myocardial infarction, one AdVEGF-B_{186}-transduced normoxic pig, and one AdVEGF-B_{186}+AdsVEGFR-1-transduced normoxic pigs. In contrast, all of the ischemic AdVEGF-B_{186}+AdsVEGFR-1 pigs (n = 6) displayed VAs 6 days after GT ($p < 0.05$). To better characterize these arrhythmias, a subset of animals received an implantable cardiac rhythm monitor on day 0, and data were collected at the time of death or at the time of sacrifice on day 6. (C) A representative example of sinus rhythm (SR) and the onset of ventricular tachycardia (VT) observed after AdVEGF-B_{186}+AdsVEGFR-1-transduced pig, is shown in Figures 3C and 3D.

To study the significance of these arrhythmias, we retrospectively analyzed data from 334 Ad GT experiments performed in our group using the same model. 12.3% of pigs died during the ischemia operation before any GT. 9.9% of the surviving animals died during the first 24 h after myocardial infarction. In these cases, the death was unlikely related to the transgene, since protein production is very low at this time point, biological effects are observed only 2–3 days after GT, and the maximal effect of Ad gene transfer is known to be at day 6. Only seven of the remaining 264 animals died 2–5 days after the GT (2.65%). Five of these pigs had received AdVEGF-B_{186} GT (four ischemic pigs, one normoxic pig), one was transduced with AdVEGF-B_{186}+AdsVEGFR-1 (ischemic), and one was unrelated to this study. All deaths were sudden cardiac deaths. AdVEGF-B_{186}, therefore, significantly increased the risk of sudden cardiac death as compared to any other therapeutic or control GT when analyzed with a log-rank test (hazard ratio, 0.001998; 95% confidence interval [CI] = 0.0001853–0.02153, $p < 0.0001$) (Figure 3E) and is the main driver of this effect.

AdVEGF-B_{186} Increases the Expression of Molecules Associated with Nerve Growth and Differentiation

To elucidate molecular mechanisms of VEGF-B-induced nerve growth, Affymetrix gene expression arrays were performed using AdVEGF-B_{186}- and AdGFP-transduced rat neonatal cardiomyocytes 24 h after transduction. A total of 624 genes were upregulated, and 240 genes were downregulated in AdVEGF-B_{186}-transduced cardiomyocytes as compared to those in AdGFP-transduced cardiomyocytes. VEGF-B regulated the expression of factors controlling nerve growth and differentiation. Upregulated transcripts included activating transcription factor 6 (ATF6; 2.1-fold as compared to AdGFP, p = 0.00084), its downstream target mesencephalic astrocyte-derived neurotrophic factor (MANF; 2.3-fold, p = 1.47E−05),[15] and the orphan nuclear receptor (Nr4a2; 8.4-fold, p = 3.10E−05). All three are known to regulate neuronal differentiation, migration, maturation, and TH synthesis in the central nervous system.[16–18] These genes have previously been linked to neuronal growth only in the

B_{186}+sVEGFR-1 GT. Two AdVEGF-B_{186}+sVEGFR-1-transduced animals and one AdVEGF-B_{186}+AdsNrp-1-transduced animal died of VF. (D) In one of the animals, the whole chain of events was documented, demonstrating VT and induction of ventricular fibrillation (VF) leading to sudden cardiac death. AdVEGF-B_{186} gene transfer increased the probability of sudden cardiac death after acute myocardial infarction. (E) A retrospective analysis of myocardial ischemia operations and Ad GT performed on pigs in our laboratory (n = 334) revealed that AdVEGF-B_{186} GT (alone or in combination with AdsVEGFR-1) increased the incidence of sudden cardiac death. Only 7 animals died 24 h to 6 days after GT; 5 of these animals had received AdVEGF-B_{186} GT, 1 had received AdVEGF-B_{186}+sVEGFR-1 GT, and 1 was unrelated to this study. A statistically significant difference between the survival of AdVEGF-B186 and that of another GT group was observed when analyzed with the log-rank test (hazard ratio, 0.001998; 95% CI = 0.0001853–0.02153, $p < 0.0001$).

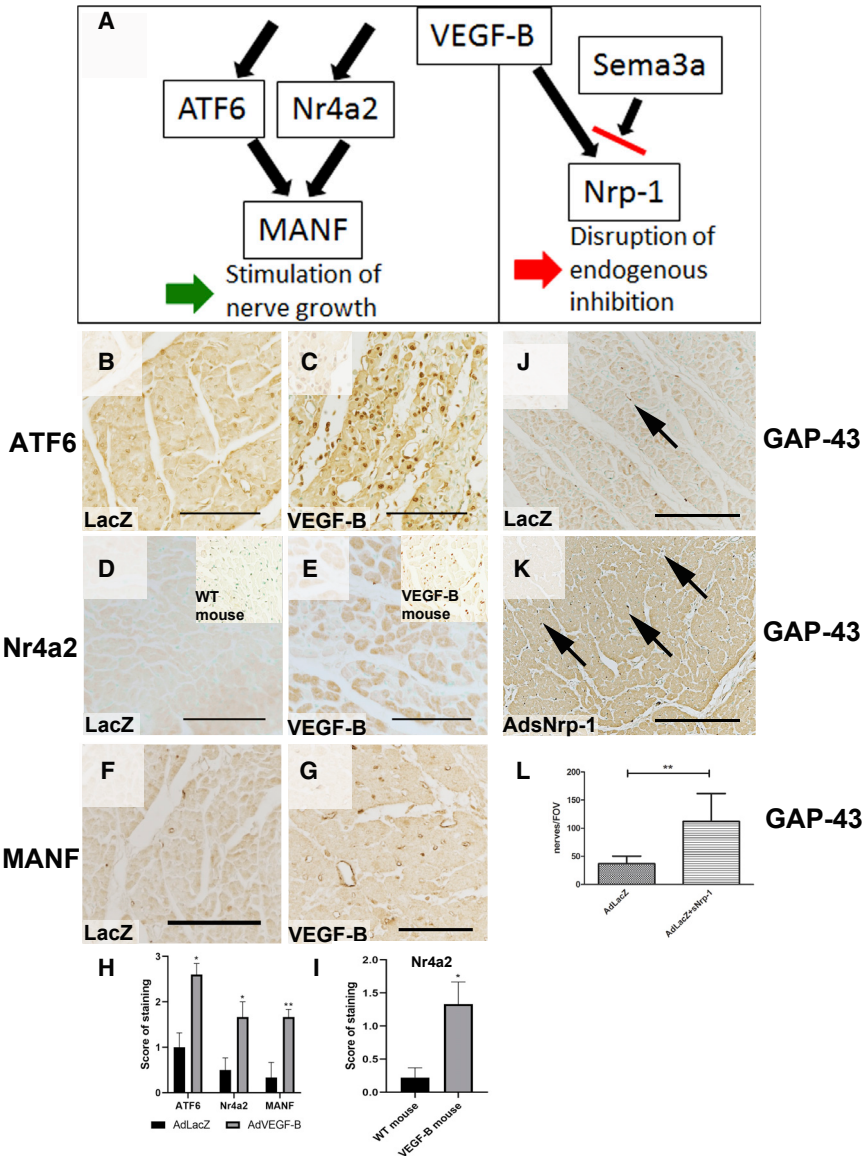

Figure 4. VEGF-B Regulates the Expression of Molecules Linked to Neuronal Growth and Differentiation

(A) The mechanism of VEGF-B-induced nerve growth. Left: VEGF-B upregulates the expression of several neurogenic molecules, including ATF6; Nr4a2; and a secreted factor, MANF. VEGF-B may, therefore, directly stimulate nerve growth via these downstream mediators. In addition, VEGF-B and soluble Nrp-1 may interfere with endogenous inhibition of nerve growth. Right: VEGF-B may compete for binding to Nrp-1 with endogenous ligands such as Sema3a, and sNrp-1 may further enhance this effect by binding Nrp-1 ligands. VEGF-B increases the expression and nuclear localization of transcription factor ATF6 6 days after Ad GT in pig myocardium ($p < 0.05$). (B and C) The nuclei were more intensely stained in VEGF-B transduced area (C) as compared to AdLacZ control GT (B). (D and E) Nuclear orphan receptor Nr4a2 expression was low in control pig myocardium (D) but was increased in AdVEGF-B_{186}-transduced pig myocardium (E) ($p < 0.05$). In addition, nuclear localization of Nr4a2 was also observed in αMHC-VEGF-B mice (insert in E), while expression level was very low in WT controls (insert in D) ($p < 0.05$). (F) The downstream target of both ATF6 and Nr4a2, MANF expression was very low in control hearts, and only a few positive cells were observed in AdLacZ-transduced pig myocardium. (G) VEGF-B increased MANF expression in capillaries and in some cardiomyocytes and other cell types ($p < 0.005$). Together, these molecules have been shown to regulate neuron growth, differentiation, and survival, thus possibly mediating the rapid nerve growth and branching observed after VEGF-B overexpression. (H and I) Immunostainings of ATF6, Nr4a2, and MANF in pig (H) and Nr4a2 in mouse (I) were analyzed blindly with semi-quantitative methods, and all were significantly increased ($p < 0.05$) in VEGF-B-overexpressing tissues. The intensity of the staining and the number of stained areas were blindly scaled from 0 to 3, with 0 representing no staining intensity, 1 representing low intensity and number of stained areas, 2 representing medium intensity and number of stained areas, and 3 representing high intensity and number of stained areas. Overexpression of AdsNrp-1 induces nerve growth in the myocardium. (J and K) AdsNrp-1 increased the number of GAP43-positive nerves 6 days after GT in pig myocardium (K) as compared to AdLacZ control (J). (L) The number of nerves per FOV was increased by 2.8-fold as compared to AdLacZ control ($p < 0.01$). This suggests that Nrp-1 has an inhibitory role in nerve patterning and that sNrp-1 disrupts this inhibitory signaling.

central nervous system. Their expression in the myocardium after acute and chronic overexpression of VEGF-B was confirmed by immunohistochemical stainings (Figure 4).

ATF6, Nr4a2, and MANF showed significant differences between the control group and the VEGF-B-overexpressing group ($p < 0.05$). ATF6 was expressed in cardiomyocytes (Figures 4B and 4C). Under baseline conditions, its expression localizes mainly in the cytoplasm, but it can translocate into the nucleus, where it functions as a transcription factor.[19] Faint ATF6 staining was observed in AdLacZ-transduced hearts (Figure 4B), while AdVEGF-B_{186} increased the staining of ATF6 (Figure 4C). Nr4a2 is a ligand-independent transcription factor shown to regulate cell differentiation, proliferation, and inhibition of apoptosis.[20] It is essential for the differentiation and maintenance of dopaminergic neurons.[21] Faint Nr4a2 staining was observed in nearly all cardiomyocyte nuclei in control hearts (Figure 4D). VEGF-B overexpression markedly increased Nr4a2 staining intensity and nuclear localization (Figure 4E). ATF6 and Nr4a2 have been shown to elicit some of their functions via MANF, a secreted factor shown to stimulate nerve growth and differentiation in the central nervous system.[22] MANF expression was very low in LacZ control hearts (Figure 4F). In AdVEGF-B_{186}-transduced hearts, MANF was strongly expressed in the endothelial cells of angiogenic capillaries and in cardiomyocytes (Figure 4G). In VEGF-B transgenic mice,

the expression was mainly seen in cardiomyocyte nuclei, and it displayed a clear endocardium-to-epicardium gradient, the expression being strongest on the endocardial side (Figure S5), possibly explaining the disturbance of the normal nerve patterning. Thus, the upregulation of transcription factors shown to stimulate nerve growth and differentiation may explain the rapid nerve sprouting observed, and upregulation of the secreted MANF protein can convey the effects of VEGF-B from transduced cardiomyocytes to surrounding nerves.

Nr4a2 also regulates Nrp-1 expression by binding directly to its promoter region,[23] and we have previously shown that VEGF-B overexpression increases Nrp-1 expression in the myocardium.[7] Nrp-1 has been shown to mediate inhibition of nerve growth by endogenous Sema3a.[4] Exogenous VEGF-B may interfere with endogenous inhibition of nerve growth mediated by Nrp-1, and VEGF-B induced nerve growth in the heart is, therefore, likely to be a result of the disruption of this negative regulation and upregulation of neurogenic molecules (Figure 4A). Accordingly, AdsNrp-1 increased GAP43-positive nerve density in the GT area (Figure 4K), as compared to AdLacZ control (Figure 4J), showing that disruption of endogenous Nrp-1 signaling is sufficient to induce nerve growth. Accordingly, nerve density was increased 2.8-fold in the AdLacZ+AdsNrp-1 group as compared to AdLacZ alone ($p = 0.0063$; Figure 4L).

DISCUSSION

In this study, we demonstrate, for the first time, that VEGF-B regulates cardiac nerve growth both during development and in the adult heart in two mammalian species. Stimulation of cardiac sympathetic innervation is mediated by the upregulation of ATF6, Nr4a2, and MANF, which are linked to nerve growth stimulation and differentation.[3]

VEGF-B Regulates Cardiac Innervation

Transgenic VEGF-B overexpression in mouse myocardium increased nerve density and loss of transmural nerve density gradient. The effect was less prominent in young mice (7–10 weeks) but became more pronounced in older animals (11–20 weeks) (Figure S1), indicating that nerves remain plastic and responsive to growth stimuli also in adults. VEGF-B has previously been linked to neurogenesis in the central nervous system[9] and regeneration of peripheral neurons.[8] Our results show, for the first time, that VEGF-B also regulates cardiac innervation, thus shedding more light on its complex functions, including the regulation of both blood vessel growth and tissue metabolism in the heart.[7,24,25]

Cardiac Nerves as a Therapeutic Target

Cardiac nerves participate in the regulation of coronary function, cardiac hypertrophy, and electromechanical activity, and thus have a profound effect on heart function. Our results indicate that modulation of cardiac innervation in the adult heart can occur upon Ad GT. Molecular tools to modify VEGF signaling are available, and GT offers a possibility to modify nerve regeneration locally. It is, thus, essential to consider the neurogenic properties of vascular growth factors in order to avoid side effects when developing novel therapies for myocardial ischemia and heart failure.

Transgenic VEGF-B overexpression increased the risk of arrhythmias during pharmacological sympathetic stimulation with dobutamine. Loss of VEGF-B in KO animals led to a modest reduction in nerve density, indicating that VEGF-B is not essential for cardiac nerve development and maintenance. This finding was confirmed in another VEGF-B KO strain,[26] with similar results (data not shown). VEGF-B KO mice have smaller hearts and dysfunctional coronary vasculature.[27] These phenotypic characteristics might be reflections of the modestly impaired cardiac innervation, as sympathetic nerves participate in the regulation of coronary function and heart growth.[28]

The αMHC-VEGF-B transgene drives the expression of both VEGF-B isoforms in cardiomyocytes, induces expansion of coronary vasculature, and leads to the development of mild cardiac hypertrophy without compromising heart function.[13] Rats expressing the same mouse VEGF-B transgene had a normal lifespan, expanded the coronary arterial tree, and showed reprogramming of cardiomyocyte metabolism that was associated with protection against myocardial infarction and preservation of mitochondrial complex I function upon ischemia reperfusion.[13] Furthermore, AAV-VEGF-B_{186} phenocopied the coronary expansion and cardiac hypertrophy in adult mice without affecting cardiac rhythm.[11,29] Thus, it is also possible that increased vasculature and hypertrophy in αMHC-VEGF-B transgenic mice sensitized these animals to arrhythmias during the dobutamine stress. In contrast, a cardiomyocyte-specific human VEGF-B_{167} transgene in mice led to increased ceramide levels in the heart[25] and later to heart failure.[30] In another study, tachypacing-induced cardiomyopathy was prevented in dogs by intracoronary AAV-VEGF-B_{167} administration without increasing mortality.[31] However, it should be taken into account that arrhythmias cannot be detected during continuous pacing.

Ad overexpression of VEGF-B_{186} led to nerve sprouting locally in the GT area in pig hearts (Figure S6). The response was rapid, and nerve density was significantly increased within days after GT, resembling endogenous nerve sprouting in the infarction border zone.[2] Increased nerve sprouting has been shown to correlate with the incidence of cardiac arrhythmias and sudden cardiac death, both in experimental animal models and in humans. Thus, in certain animal models, Ad overexpression of VEGF-B_{186} has not been beneficial, since it can cause hypertrophy and increase the risk of arrhythmias. Accordingly, retrospective survival analysis of 334 GT experiments in pigs revealed that AdVEGF-B_{186} GT significantly increased the risk of sudden cardiac death.

The co-transduction of AdVEGF-B_{186} and AdsVEGFR-1 did not affect nerve density in the GT area but did increase the risk of arrhythmias. Furthermore, very high doses of AdGT might increase the risk of arrhythmias. Ventricular extrasystoles and non-sustained

ventricular tachycardias were observed in all ischemic pigs in this group. We have previously shown that AdsVEGFR-1 efficiently blocks the vascular response of AdVEGF-B_{186}, indicating that AdsVEGFR-1 binds to VEGF-B and is capable of inhibiting its angiogenic properties.[7] AdsVEGFR-1 may, therefore, potentiate the neurogenic effects of VEGF-B by inhibiting its binding to native VEGFR-1 while allowing its binding to Nrp-1.

Co-transduction with AdsNrp-1 significantly enhanced nerve sprouting as compared to AdVEGF-B_{186} alone. A similar effect has been observed in angiogenesis, where sNrp-1 enhances the angiogenic effect of VEGF-A, likely by acting as a co-receptor and increasing VEGF-A binding to VEGFR-2.[32,33] As VEGF-B does not bind to VEGFR-2, and VEGFR-1-mediated signaling did not appear essential for nerve sprouting, sNrp-1 may enhance nerve growth by the binding endogenous inhibitory ligand of Nrp-1, Sema3a. Sema3a has been shown to inhibit nerve growth in the heart both during development and in ischemia.[4,34] Sema3a overexpression also protects from arrhythmias after myocardial ischemia.[34] The effects of VEGF-B seem to be the opposite, suggesting that VEGF-B may block inhibitory signaling via native Nrp-1. Our finding further supports this hypothesis that AdsNrp-1 alone is sufficient to induce nerve growth in the heart.

Gene expression analysis revealed that VEGF-B regulates the expression of several molecules previously linked to neurogenesis, neuronal differentiation, and survival in the central nervous system. ATF6 was upregulated along with its known downstream targets, MANF[15] and Nr4a2. This pathway has been shown to regulate neuronal differentiation, migration, maturation, and TH synthesis in the central nervous system.[16–18] MANF has also been shown to be expressed in the myocardium and to mediate cardioprotective effects.[15,35] MANF is secreted from cardiomyocytes and may, therefore, mediate signaling from cardiomyocytes to neurons. Further studies are required to confirm whether MANF upregulation is essential in mediating VEGF-B-induced nerve growth. Nr4a2 upregulation may also mediate the Nrp-1 upregulation shown in our previous study,[7] as Nr4a2 has been shown to directly regulate Nrp-1 expression in dopaminergic neurons.[23]

The role of VEGF-B in endogenous sympathetic dysregulation in the human heart remains unclear. VEGF-B is expressed in the human myocardium, but expression level and localization are not known. Both genetic and Ad overexpression of VEGF-B lead to very high expression levels. However, these effects may not reflect the endogenous role of the growth factor, although, these models provide tools to manipulate nerve growth in the heart and to study the functional and electrophysiological consequences of nerve sprouting.

In this study, we show, for the first time, that VEGF-B regulates cardiac innervation in the adult heart. Nerve sprouting leads to an increased risk of arrhythmias and sudden cardiac death in dobutamine-stressed hearts. We also show that VEGF-B regulates the expression of three genes in the neurogenic pathway and provide evidence that disruption of the endogenous Nrp-1 signaling has arrhythmogenic effects. Local modulation of nerve growth after myocardial ischemia using GT approaches may provide a novel treatment strategy to prevent postischemic arrhythmias as well as allow the use of VEGF-B gene transfer as a potential treatment for myocardial ischemia.

Clinical Relevance

Nerve growth and angiogenesis share common molecular regulators, such as VEGF-B, and occur as part of the endogenous repair process after myocardial ischemia. Sympathetic nerve growth and abnormal nerve distribution in the heart induced by VEGF-B increased the risk of arrhythmias and sudden cardiac death. Identification of the VEGFR-1-independent pathogenic mechanisms and patients with abnormal sympathetic activity may help to identify high-risk patients.[36] This may also allow the development of specific proangiogenic and antiarrhythmic therapies for the treatment of myocardial ischemia and post-ischemic arrhythmias.

MATERIALS AND METHODS

Animal Models

All animal procedures were approved by The National Animal Experimental Board of Finland and carried out in accordance with the guidelines of The Finnish Act on Animal Experimentation. Animals were kept in standard housing conditions in The National Laboratory Animal Center of The University of Eastern Finland, Kuopio, Finland. Diet and water were provided *ad libitum*.

Transgenic female mice expressing the VEGF-B gene selectively under αMHC-VEGF-B,[11] VEGF-B KO mice,[27] and their WT littermates were used to study the effects of chronic VEGF-B overexpression on nerve-ending density and distribution (Table S2). In preliminary studies, we found no difference between sexes; therefore, it is justified to use only female mice, as they were more readily available. Moreover, the pig studies were also made in female pigs, making the comparison between the species more straightforward.

Surface ECG recordings (lead II via limb electrodes) were performed with the Vevo 2100 Ultrasound System designed for small animals (Fujifilm VisualSonics, Toronto, ON, Canada). Myocardial samples were collected for histological analysis. A subset of animals (n = 10 in each group) was subjected to dobutamine stress (1 mg/kg, i.p. injection), and the occurrence of arrhythmias was observed 5, 10, and 15 min after the onset of dobutamine infusion.

AdVEGF-B_{186} was used to study the short-term effects of VEGF-B in pig myocardium (Table S2). A dose of 1×10^{12} virus particles(vp)/mL of AdLacZ as a negative control, AdVEGF-B_{186} alone or in combination with sVEGFR-1,[37] or soluble Nrp-1 (sNrp-1) was injected intramyocardially (10× 200-μL injections) into the anterolateral wall of the left ventricle using a NOGA Myostar injection catheter (Biosense Webster, Johnson & Johnson, Irvine, CA, USA).[38] In a subset of animals, acute myocardial infarction was induced at baseline as previously described,[7] and the GT was done 30 min after the infarction was established for these animals. A VortX-18 occlusion coil (Boston

Scientific, Marlborough, MA, USA) was carefully placed at the similar position of the left anterior descending coronary artery for each pig. A lower dose of Ad was used (5×10^9 vp/mL), as ischemia induces expression of endogenous growth factors and potentiates the effects of VEGFs as previously described.[34] Surface ECG (leads I, II, and III) (Zoll, Chelmsford, MA, USA) was recorded at baseline and 6 days after GT or with implantable rhythm monitors (Reveal LINQ ICM System, Medtronic, Minneapolis, MN, USA) (Table S2). Evans blue dye (30 mg/mL in saline, 1 mL/kg; E2129, Sigma-Aldrich, St. Louis, MO, USA) was injected intravenously to visualize the injection sites, and myocardial samples were collected for histological analyses.

We conducted a retrospective analysis of myocardial ischemia operations and Ad GT performed on pigs in our laboratory (n = 334). The data were collected from our groups' archives. Data were divided into two groups: normoxic (n = 83) and ischemic (n = 251) pigs. Calculations were divided into three time periods: during the ischemia operation before any GT (day 0), 24 h after GT (day 1), and 2–5 days after ischemia (days 2–5). Day 1 was chosen because the death on that day was unlikely to be related to the transgene, since protein production is minimal at this time point. Days 2–5 are more likely related to transgene, as the biological effects are observed 2–3 days after GT, and maximal gene expression is on day 6, which was the sacrification day.

Detection of Arrhythmias

Mouse ECG recordings were analyzed with Kubios murine software as previously described.[39] Pig ECG recordings were analyzed manually from printed recordings in a blinded manner. Both premature ventricular extrasystoles and non-sustained ventricular tachycardias were characterized as arrhythmias.

Gene Expression Arrays

To study the molecular mechanism behind VEGF-B-induced nerve growth, Affymetrix gene expression arrays were used (Table S1). Rat neonatal cardiomyocytes were isolated, and 24 h later, the cells were transduced with either negative-control AdGFP or AdVEGF-B_{186} (MOI = 10). Cells were collected 24 h later, RNA was isolated, and Affymetrix gene expression arrays were performed at the Dana Farber Cancer Institute core facility. Rats were used, as it is a mammalian species with a cardiovascular system very similar to that of humans. Also, rat is the only species from which large amounts of cardiomyocytes can be obtained for *in vitro* studies. Generally, data derived from rat cardiomyocytes have been regarded to represent very well *in vivo* situations in mice, humans, and other mammalian species.

Gene expression microarray data were analyzed using the R statistical package, v.2.13. Microarray probe sets were mapped using custom CDF files (RaGene10stv1, v.14.1.0), and the Robust Multi-Array Average expression measure was used to normalize the data. Quality assessment of the microarrays was performed using the following Bioconductor packages: affy, v.1.3; affyPLM, v.1.28.5; and affyQCReport, v.1.3. Based on the quality assessment, all microarrays advanced to further analysis. Non-specific filtering was used to filter out probe sets that did not map to known genes as well as to remove duplicate probe sets mapped to the same gene (the probe set with the most variability across the microarrays was retained). After the filtering of the original 19,239 probe sets, 19,225 probe sets representing gene expression values for the same number of unique genes were retained for further analysis.

The Linear Models for Microarray Data (limma) v.3.8.1 analysis package was used to detect differentially expressed genes between groups, using fitting of linear models and applying empirical Bayes smoothing to each probe. The Benjamini-Hochberg false discovery rate (FDR) was used to adjust results for multiple comparisons. A FDR-adjusted p value < 0.05 was considered as statistically significant.

Gene set enrichment analysis (GSEA) of significantly differentially expressed genes was performed to identify over-represented Gene Ontology (GO) terms and Kyoto Encyclopedia of Genes and Genomes (KEGG) pathways. The hypergeometric test from the Bioconductor Category package, v.2.18, was used for enrichment analysis. In addition, GSEA was used to identify enriched gene sets from the results of differentially expressed gene analyses. For the GSEA, the rat genes were mapped to the closest corresponding orthologous human genes using Ensembl Biomart (Ensembl Genes v.62). Lists of the human genes ranked by fold change were used. Enrichment of GO biological process terms and different pathway gene sets (Biocarta, KEGG, and Reactome) were studied. Gene sets were obtained from MSigDB v.3. Gene sets smaller than 15 and larger than 500 terms were excluded. Gene sets with a FDR q value < 0.25 were considered as statistically significantly enriched gene sets.

Immunohistochemistry

Hearts were rinsed from blood with PBS, and perfusion was fixed with 1% paraformaldehyde (PFA) in PBS (mice) or with 1% PFA in citrate buffer to improve Evans blue retention in the tissues (pigs). Myocardial samples were further immersion-fixed in 4% PFA overnight and embedded in paraffin. 7-μm sections were used for histological analyses. GAP43 (AB5220, Millipore, Burlington, MA, USA; dilution 1:100) was used to visualize sprouting nerve endings, and TH staining was used to confirm the sympathetic nature of these nerves (AB1542, Millipore, Burlington, MA, USA; dilution 1:100 for tissue sections and 1:500 for whole-mount samples). Nurr1/Nr4a2 (AB93332, Abcam, UK; dilution 1:100), ATF6 (NBP1-40256, Novus Biologicals, Centennial, CO, USA; dilution 1:100) and MANF (sc-34560, Santa Cruz Biotechnology, Santa Cruz, CA, USA; dilution 1:100) were used to visualize upregulation of VEGF-B target proteins in myocardial sections. DAB (Vector Laboratories, Burlingame, CA, USA) was used to visualize the staining, and Methyl Green (S1962, DAKO, Santa Clara, CA, USA) was used as a counterstain.

The intensity of the stainings and the number of stained areas were scored blindly using a scale ranging from 0 to 3, where 0 indicates

no staining intensity, 1 indicates low intensity and number of stained areas, 2 indicates medium intensity and number of stained areas, and 3 indicates high intensity and number of stained areas.40

Nerve-ending density was quantified from both GAP43-stained sections with AnalySIS software (Soft Imaging System, Münster, Germany), and the number of nerves per FOV was counted. 5 FOVs per section at magnification of 200× immediately adjacent to the needle track were used for analysis.

Statistical Analysis

A two-way ANOVA with Bonferroni posttests (nerve ending densities in mouse heart; Figure 1) and a one-way ANOVA with Tukey's multiple comparison test were used to achieve the most reliable statistical analysis, as they can control overall type 1 error, meaning that false-positive results can also be controlled, especially in the small-group-size studies (nerve densities in pig myocardium, Figure 2). A chi-square test (arrhythmia differences; Figure 3), Student's t test (nerve ending density in pig myocardium; AdLacZ versus AdLacZ +AdsNrp-1; Figures 4J and 4K), and Mann-Whitney U test (the difference between groups as shown in Figures 4B–4G) were used to evaluate the statistical significance of the findings. Significance of the occurrence of sudden cardiac death was analyzed using a log-rank test (Figure 3). A p value of <0.05 was considered statistically significant.

SUPPLEMENTAL INFORMATION

Supplemental Information can be found online at https://doi.org/10.1016/j.ymthe.2020.03.011.

AUTHOR CONTRIBUTIONS

J.L. and O-P.H. conducted most of the experiments, designed the experiments, and wrote the paper. A.K. took part in most large animal experiments. J.H. took part in some of the mouse experiments. J.P. conducted most of the biostatistical analysis. M.L. and J.N. took part in some of the animal studies, the manuscript-writing process, and the design of the study. M.H., N.L-K., P.M., and J.H. provided crucial information regarding data analysis and experimental design. M.R., J.N., and K.A. took part in visualization and the review and editing of the manuscript, as well as helped design experiments. A.R. conducted supervision and provided some resources for the study. S.Y.-H. conducted supervision and funding acquisition and conducted the writing, editing, and reviewing of the manuscript as well as the design of the study.

CONFLICTS OF INTEREST

The authors declare no competing interests.

ACKNOWLEDGMENTS

This study was supported by grants from the Finnish Foundation for Cardiovascular Research, ERC, and the Finnish Academy Center of Excellence on Cardiovascular and Metabolic Diseases. The authors want to thank the staff at the Laboratory Animal Center—especially Heikki Karhunen, Minna Törrönen, and Riikka Venäläinen—and technicians Sari Järveläinen and Tiina Koponen of the National Virus Vector Laboratory, Biocenter Kuopio and EU-EATRIS infrastructure for Ad production. Dr. Riikka Kivelä is acknowledged for her comments and suggestions during the preparation of the manuscript.

REFERENCES

1. Cao, J.M., Fishbein, M.C., Han, J.B., Lai, W.W., Lai, A.C., Wu, T.J., Czer, L., Wolf, P.L., Denton, T.A., Shintaku, I.P., et al. (2000). Relationship between regional cardiac hyperinnervation and ventricular arrhythmia. Circulation *101*, 1960–1969.

2. Oh, Y.S., Jong, A.Y., Kim, D.T., Li, H., Wang, C., Zemljic-Harpf, A., Ross, R.S., Fishbein, M.C., Chen, P.S., and Chen, L.S. (2006). Spatial distribution of nerve sprouting after myocardial infarction in mice. Heart Rhythm *3*, 728–736.

3. Chen, P.S., Chen, L.S., Cao, J.M., Sharifi, B., Karagueuzian, H.S., and Fishbein, M.C. (2001). Sympathetic nerve sprouting, electrical remodeling and the mechanisms of sudden cardiac death. Cardiovasc. Res. *50*, 409–416.

4. Ieda, M., Kanazawa, H., Kimura, K., Hattori, F., Ieda, Y., Taniguchi, M., Lee, J.K., Matsumura, K., Tomita, Y., Miyoshi, S., et al. (2007). Sema3a maintains normal heart rhythm through sympathetic innervation patterning. Nat. Med. *13*, 604–612.

5. Zhou, S., Chen, L.S., Miyauchi, Y., Miyauchi, M., Kar, S., Kangavari, S., Fishbein, M.C., Sharifi, B., and Chen, P.S. (2004). Mechanisms of cardiac nerve sprouting after myocardial infarction in dogs. Circ. Res. *95*, 76–83.

6. Lohela, M., Bry, M., Tammela, T., and Alitalo, K. (2009). VEGFs and receptors involved in angiogenesis versus lymphangiogenesis. Curr. Opin. Cell Biol. *21*, 154–165.

7. Lähteenvuo, J.E., Lähteenvuo, M.T., Kivelä, A., Rosenlew, C., Falkevall, A., Klar, J., Heikura, T., Rissanen, T.T., Vähäkangas, E., Korpisalo, P., et al. (2009). Vascular endothelial growth factor-B induces myocardium-specific angiogenesis and arteriogenesis via vascular endothelial growth factor receptor-1- and neuropilin receptor-1-dependent mechanisms. Circulation *119*, 845–856.

8. Guaiquil, V.H., Pan, Z., Karagianni, N., Fukuoka, S., Alegre, G., and Rosenblatt, M.I. (2014). VEGF-B selectively regenerates injured peripheral neurons and restores sensory and trophic functions. Proc. Natl. Acad. Sci. USA *111*, 17272–17277.

9. Sun, Y., Jin, K., Childs, J.T., Xie, L., Mao, X.O., and Greenberg, D.A. (2006). Vascular endothelial growth factor-B (VEGFB) stimulates neurogenesis: evidence from knockout mice and growth factor administration. Dev. Biol. *289*, 329–335.

10. Jensen, L.D., Nakamura, M., Bräutigam, L., Li, X., Liu, Y., Samani, N.J., and Cao, Y. (2015). VEGF-B-Neuropilin-1 signaling is spatiotemporally indispensable for vascular and neuronal development in zebrafish. Proc. Natl. Acad. Sci. USA *112*, E5944–E5953.

11. Kivelä, R., Bry, M., Robciuc, M.R., Räsänen, M., Taavitsainen, M., Silvola, J.M., Saraste, A., Hulmi, J.J., Anisimov, A., Mäyränpää, M.I., et al. (2014). VEGF-B-induced vascular growth leads to metabolic reprogramming and ischemia resistance in the heart. EMBO Mol. Med. *6*, 307–321.

12. Meiri, K.F., Pfenninger, K.H., and Willard, M.B. (2006). Growth-associated protein, GAP-43, a polypeptide that is induced when neurons extend axons, is a component of growth cones and corresponds to pp46, a major polypeptide of a subcellular fraction enriched in growth cones. Proc. Natl. Acad. Sci. USA *83*, 3537–3541.

13. Bry, M., Kivelä, R., Holopainen, T., Anisimov, A., Tammela, T., Soronen, J., Silvola, J., Saraste, A., Jeltsch, M., Korpisalo, P., et al. (2010). Vascular endothelial growth factor-B acts as a coronary growth factor in transgenic rats without inducing angiogenesis, vascular leak, or inflammation. Circulation *122*, 1725–1733.

14. McLenachan, J.M., Henderson, E., Morris, K.I., and Dargie, H.J. (1987). Ventricular arrhythmias in patients with hypertensive left ventricular hypertrophy. N. Engl. J. Med. *317*, 787–792.

15. Tadimalla, A., Belmont, P.J., Thuerauf, D.J., Glassy, M.S., Martindale, J.J., Gude, N., Sussman, M.A., and Glembotski, C.C. (2008). Mesencephalic astrocyte-derived neurotrophic factor is an ischemia-inducible secreted endoplasmic reticulum stress response protein in the heart. Circ. Res. *103*, 1249–1258.

16. Alavian, K.N., Jeddi, S., Naghipour, S.I., Nabili, P., Licznerski, P., and Tierney, T.S. (2014). The lifelong maintenance of mesencephalic dopaminergic neurons by Nurr1 and engrailed. J. Biomed. Sci. *21*, 27.

17. Zhang, T., Jia, N., Fei, E., Wang, P., Liao, Z., Ding, L., Yan, M., Nukina, N., Zhou, J., and Wang, G. (2007). Nurr1 is phosphorylated by ERK2 in vitro and its phosphorylation upregulates tyrosine hydroxylase expression in SH-SY5Y cells. Neurosci. Lett. *423*, 118–122.

18. Lindahl, M., Saarma, M., and Lindholm, P. (2017). Unconventional neurotrophic factors CDNF and MANF: structure, physiological functions and therapeutic potential. Neurobiol. Dis. *97* (Pt B), 90–102.

19. Glembotski, C.C. (2014). Roles for ATF6 and the sarco/endoplasmic reticulum protein quality control system in the heart. J. Mol. Cell. Cardiol. *71*, 11–15.

20. Zhao, Y., and Bruemmer, D. (2010). NR4A orphan nuclear receptors: transcriptional regulators of gene expression in metabolism and vascular biology. Arterioscler. Thromb. Vasc. Biol. *30*, 1535–1541.

21. Caiazzo, M., Dell'Anno, M.T., Dvoretskova, E., Lazarevic, D., Taverna, S., Leo, D., Sotnikova, T.D., Menegon, A., Roncaglia, P., Colciago, G., et al. (2011). Direct generation of functional dopaminergic neurons from mouse and human fibroblasts. Nature *476*, 224–227.

22. Glembotski, C.C., Thuerauf, D.J., Huang, C., Vekich, J.A., Gottlieb, R.A., and Doroudgar, S. (2012). Mesencephalic astrocyte-derived neurotrophic factor protects the heart from ischemic damage and is selectively secreted upon sarco/endoplasmic reticulum calcium depletion. J. Biol. Chem. *287*, 25893–25904.

23. Hermanson, E., Borgius, L., Bergsland, M., Joodmardi, E., and Perlmann, T. (2006). Neuropilin1 is a direct downstream target of Nurr1 in the developing brain stem. J. Neurochem. *97*, 1403–1411.

24. Hagberg, C.E., Mehlem, A., Falkevall, A., Muhl, L., Fam, B.C., Ortsäter, H., Scotney, P., Nyqvist, D., Samén, E., Lu, L., et al. (2012). Targeting VEGF-B as a novel treatment for insulin resistance and type 2 diabetes. Nature *490*, 426–430.

25. Karpanen, T., Bry, M., Ollila, H.M., Seppänen-Laakso, T., Liimatta, E., Leskinen, H., Kivelä, R., Helkamaa, T., Merentie, M., Jeltsch, M., et al. (2008). Overexpression of vascular endothelial growth factor-B in mouse heart alters cardiac lipid metabolism and induces myocardial hypertrophy. Circ. Res. *103*, 1018–1026.

26. Aase, K., von Euler, G., Li, X., Pontén, A., Thorén, P., Cao, R., Cao, Y., Olofsson, B., Gebre-Medhin, S., Pekny, M., et al. (2001). Vascular endothelial growth factor-B-deficient mice display an atrial conduction defect. Circulation *104*, 358–364.

27. Bellomo, D., Headrick, J.P., Silins, G.U., Paterson, C.A., Thomas, P.S., Gartside, M., Mould, A., Cahill, M.M., Tonks, I.D., Grimmond, S.M., et al. (2000). Mice lacking the vascular endothelial growth factor-B gene (Vegfb) have smaller hearts, dysfunctional coronary vasculature, and impaired recovery from cardiac ischemia. Circ. Res. *86*, E29–E35.

28. Tucker, D.C., and Gist, R. (1986). Sympathetic innervation alters growth and intrinsic heart rate of fetal rat atria maturing in oculo. Circ. Res. *59*, 534–544.

29. Räsänen, M., Degerman, J., Nissinen, T.A., Miinalainen, I., Kerkelä, R., Siltanen, A., Backman, J.T., Mervaala, E., Hulmi, J.J., Kivelä, R., and Alitalo, K. (2016). VEGF-B gene therapy inhibits doxorubicin-induced cardiotoxicity by endothelial protection. Proc. Natl. Acad. Sci. USA *113*, 13144–13149.

30. Lottonen-Raikaslehto, L., Rissanen, R., Gurzeler, E., Merentie, M., Huusko, J., Schneider, J.E., Liimatainen, T., and Ylä-Herttuala, S. (2017). Left ventricular remodeling leads to heart failure in mice with cardiac-specific overexpression of VEGF-B_{167}: echocardiography and magnetic resonance imaging study. Physiol. Rep. *5*, e13096.

31. Pepe, M., Mamdani, M., Zentilin, L., Csiszar, A., Qanud, K., Zacchigna, S., Ungvari, Z., Puligadda, U., Moimas, S., Xu, X., et al. (2010). Intramyocardial VEGF-B167 gene delivery delays the progression towards congestive failure in dogs with pacing-induced dilated cardiomyopathy. Circ. Res. *106*, 1893–1903.

32. Kivelä, R., Hemanthakumar, K.A., Vaparanta, K., Robciuc, M., Izumiya, Y., Kidoya, H., Takakura, N., Peng, X., Sawyer, D.B., Elenius, K., et al. (2019). Endothelial cells regulate physiological cardiomyocyte growth via VEGFR2-mediated paracrine signaling. Circulation *139*, 2570–2584.

33. Yamada, Y., Takakura, N., Yasue, H., Ogawa, H., Fujisawa, H., and Suda, T. (2001). Exogenous clustered neuropilin 1 enhances vasculogenesis and angiogenesis. Blood *97*, 1671–1678.

34. Hu, H., Xuan, Y., Xue, M., Cheng, W., Wang, Y., Li, X., Yin, J., Li, X., Yang, N., Shi, Y., and Yan, S. (2016). Semaphorin 3A attenuates cardiac autonomic disorders and reduces inducible ventricular arrhythmias in rats with experimental myocardial infarction. BMC Cardiovasc. Disord. *16*, 16.

35. Glembotski, C.C. (2011). Functions for the cardiomyokine, MANF, in cardioprotection, hypertrophy and heart failure. J. Mol. Cell. Cardiol. *51*, 512–517.

36. Ylä-Herttuala, S., Bridges, C., Katz, M.G., and Korpisalo, P. (2017). Angiogenic gene therapy in cardiovascular diseases: dream or vision? Eur. Heart J. *38*, 1365–1371.

37. Sallinen, H., Anttila, M., Narvainen, J., Koponen, J., Hamalainen, K., Kholova, I., Heikura, T., Toivanen, P., Kosma, V.M., Heinonen, S., et al. (2009). Antiangiogenic gene therapy with soluble VEGFR-1, -2, and -3 reduces the growth of solid human ovarian carcinoma in mice. Mol. Ther. *17*, 278–284.

38. Nurro, J., Halonen, P.J., Kuivanen, A., Tarkia, M., Saraste, A., Honkonen, K., Lähteenvuo, J., Rissanen, T.T., Knuuti, J., and Ylä-Herttuala, S. (2016). AdVEGF-B186 and AdVEGF-DΔNΔC induce angiogenesis and increase perfusion in porcine myocardium. Heart *102*, 1716–1720.

39. Merentie, M., Lipponen, J.A., Hedman, M., Hedman, A., Hartikainen, J., Huusko, J., Lottonen-Raikaslehto, L., Parviainen, V., Laidinen, S., Karjalainen, P.A., and Ylä-Herttuala, S. (2015). Mouse ECG findings in aging, with conduction system affecting drugs and in cardiac pathologies: development and validation of ECG analysis algorithm in mice. Physiol. Rep. *3*, 1–13.

40. Bräsen, J.H., Häkkinen, T., Malle, E., Beisiegel, U., and Ylä-Herttuala, S. (2003). Patterns of oxidized epitopes, but not NF-κ B expression, change during atherogenesis in WHHL rabbits. Atherosclerosis *166*, 13–21.